Finitely large phased arrays of microstrip antennas : analysis and design

Preface

The paper in this RANA report has been submitted to the proceedings of the 4th International Workshop "Scientific Computing in Electrical Engineering" (SCEE). This workshop was organized by the Eindhoven University of Technology from the 23th till the 28th of June, 2002. A poster about the research described in the paper was presented at this workshop. Details are described in two internal reports of Thales Nederland B.V., namely "Finitely Large Phased Arrays of Microstrip Antennas" by D.J. Bekers (EAR 9501 027 223) and "A Planar Array of Narrow Ring-Shaped Microstrips in Half Space" by W. Dijkstra (EAR 9501 027 224).

Finitely Large Phased Arrays of Microstrip Antennas – Analysis and Design

Dave J. Bekers[1], Stef J.L. van Eijndhoven, Alphons A.F. van de Ven, Peter-Paul Borsboom[2], and Evert W. Kolk[3]

[1] Eindhoven University of Technology, Department of Mathematics and Computer Science, P.O. Box 513, 5600 MB Eindhoven, The Netherlands
[2] Thales Nederland B.V., Department JRS, P.O. Box 42, 7550 GD Hengelo, The Netherlands
[3] Thales Air Defense, Haneau de Roussigny, 91470 Limours, France

Abstract. This paper focuses on the development of a model to obtain qualitative insight in the behaviour of large, but finite, phased arrays of microstrip antennas. This model concerns a finite array of simple elements, namely perfectly conducting, infinitely thin, narrow rings, excited by voltage gaps and positioned in free or half space. The currents on the rings, and from that the electromagnetic field, are calculated by a moment method. Dimension analysis is carried out to reduce numerical effort and to acquire insight in the behaviour of the array. The qualitative analysis shows promising results and although numerically a brute force method has been applied, CPU times are still acceptable.

1 Problem Description

Currently, Thales Nederland is realizing new radar systems consisting of large phased arrays of microstrip antennas. These arrays consist of about 1000 antenna elements positioned on an antenna face of about $16\,\mathrm{m}^2$. The systems scan in azimuth by rotation and in elevation by phase shifts. A narrow main lobe and low side lobe level, an impedance match with the feeding network of the array, and a low cross polarization are design goals.

To analyse such arrays, either a finite array model (or element-by-element approach) or an infinite array model is used at Thales Nederland. The infinite array model requires much less computation time and data storage demand than the finite array model. However, since it cannot account for edge effects and differences between the antenna elements, the need for a finite array model still exists to meet the design goals.

Since the actual geometry of the antenna elements is complicated, simulation of a finite array taking into account in detail these elements will require too much computing resources to be realistically feasible. Therefore, we have decided to develop a model based on simple elements that will enable us to find the characteristics that describe the qualitative behaviour of large phased arrays.

2 Modelling

The main requirements on our model are the following. Firstly, the arrays are finite such that boundary effects can be incorporated. Secondly, computation times should be in the order of hours. Thirdly, the algorithm should be based on analytical expressions to provide insight in the characteristics or characteristic parameters of an array.

The qualitative model concerns a finite planar array of simple elements in free space or above an infinitely wide ground plate. Considering the radiating part of the actual antenna elements, i.e. a rectangular microstrip loop, we have chosen perfectly conducting, infinitely thin, narrow ring-shaped microstrips, shortly rings, as elements; see Fig. 1. The reasons for this choice are twofold. A ring is the most simple loop geometry and the modes on this geometry can be described analytically.

The rings are excited by voltage gaps at a certain frequency with corresponding wavelength λ and wave number k. On each ring, the gap is uniform with respect to the width and can be positioned arbitrarily. The widths $2b_q$ of the rings are all of the same order, but much smaller than the wavelength, the radii a_q, and the distances between the rings. In other words, $kb_q \ll 1$, $\beta_q = b_q/a_q \ll 1$, and $b_p/(L_{pq} - a_p - a_q) \ll 1$, where L_{pq} is the distance between the centers $\mathbf{c}_p$ and $\mathbf{c}_q$ of ring p and q; see Fig. 1. If a ground plate is present, the rings are situated above this plate at height h.

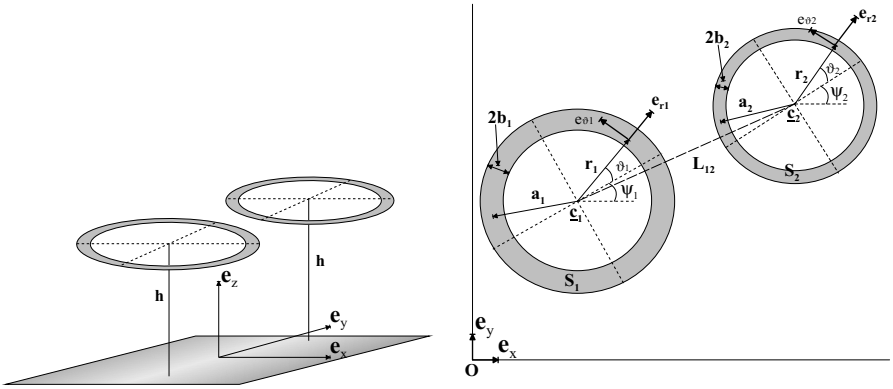

Fig. 1. Geometry of an array of two rings.

Since the excitation is time harmonic, the electromagnetic field is so also, and therefore, a (spatial) time-harmonic representation of this field is used. The time dependence is suppressed. The total electric field is written as the sum of a scattered electric field $\mathbf{E}^{scat}$ and an excitation field $\mathbf{E}^{ex}$. The scattered electric field is expressed in terms of the unknown current density

J on the rings by an integro-differential operator acting on the current,

$$\mathbf{E}^{scat} = \mathcal{L}\mathbf{J}. \tag{1}$$

The operator $\mathcal{L}$ can be factorized as $\mathcal{L} = \mathcal{D}\mathcal{T}$, where $\mathcal{D}$ is the differential operator $-j\omega\mu(\mathcal{I}+\nabla\nabla\cdot)$ and $\mathcal{T}$ is the integral operator described by a Green's kernel, where $\mathcal{T}\mathbf{J}$ is the magnetic vector potential. The condition that the tangential component of the total electric field is zero at the surface S of the rings yields an equation for the current,

$$(\mathcal{L}\mathbf{J})_{tan} = -(\mathbf{E}^{ex})_{tan}, \qquad \text{on } S. \tag{2}$$

Here, $(\,\cdot\,)_{tan}$ is a trace operator that restricts a vector field to the surface S and projects this field tangentially on S. Equation (2) is solved by a moment method expanding the unknown current into a finite number of expansion functions with unknown coefficients. Once the current is known, the electromagnetic far field can be calculated analytically.

3 Analytical Aspects

Let the surface of the q-th ring be S_q. On each S_q, a polar parameter representation is chosen, the orientation of which is described by the angle ψ_q; see Figure 1. The voltage gap on S_q is positioned in $\vartheta_q = \pi$. Hence, ψ_q determines not only the orientation of the parameter representation, but also the position of the gap. Two tangent vectors $\mathbf{e}_{r_q}$ and $\mathbf{e}_{\vartheta_q}$ correspond in the usual way to this representation. Together with the corresponding normal, they form a local coordinate system on S_q, which is extended straightforwardly to global coordinate system.

It is assumed that the current $\mathbf{J}_q = \mathbf{J}|_{S_q}$ is directed along the centerlines of the rings and that it is uniform with respect to the width b_q,

$$\mathbf{J}_q(r_q, \vartheta_q) = w(\vartheta_q)\mathbf{e}_{\vartheta_q}. \tag{3}$$

The basis of this assumption is that the wavelength is much larger than the widths of the rings. Expressing $\mathcal{L}\mathbf{J}_q$, i.e. the scattered electric field induced by ring q, into the system of S_p, we calculate $(\mathcal{L}\mathbf{J}_q)_{tan}$ on S_p straightforwardly by putting the axial coordinate equal to zero and omitting the axial component. Then, a differential operator $\mathcal{D}_{r_p\vartheta_p}$ is determined such that

$$(\mathcal{L}\mathbf{J}_q)_{tan}|_{S_p} = \mathcal{D}_{r_p\vartheta_p}(\mathcal{T}\mathbf{J}_q\big|_{S_p}), \tag{4}$$

where $|_{S_p}$ denotes the restriction to S_p. Hence, the projection of the trace operator is incorporated in $\mathcal{D}_{r_p\vartheta_p}$.

The impedance matrix component for a test function $\mathbf{v}_p$ and an expansion function $\mathbf{J}_q$ is given by

$$<\mathbf{v}_p, (\mathcal{L}\mathbf{J}_q)_{tan}|_{S_p}>, \tag{5}$$

where $<\cdot,\cdot>$ is the inner product on functions defined from S to the tangent space of S. It is shown that the variation of $(\mathcal{L}\mathbf{J}_q)_{tan}|_{S_p}$ in r_p is of order β_p with respect to its variation in ϑ_p. This implies that $(\mathcal{L}\mathbf{J}_q)_{tan}|_{S_p}$ depends only weakly on r_p. Therefore, the test function $\mathbf{v}_p$ is chosen uniform with respect to r_p and tangentially directed only. This means

$$\mathbf{v}_p(r_p, \vartheta_p) = v(\vartheta_p)\mathbf{e}_{\vartheta_p}. \tag{6}$$

Then, the impedance matrix component (5) turns into

$$<\mathbf{v}_p, (\mathcal{L}\mathbf{J}_q)_{tan}|_{S_p}> = \int_{\vartheta_p} v_p(\vartheta_p) \int_{r_p} (\mathcal{D}_{r_p\vartheta_p}[\mathcal{T}\mathbf{J}_q|_{S_p}])_{\vartheta_p}\, d\sigma(r_p, \vartheta_p). \tag{7}$$

Neglecting terms of order β_p, we reverse the differential operator $\mathcal{D}_{r_p\vartheta_p}$ and the integral with respect to r_p. This leads to averaging of the Green's kernel with respect to the radial source and observation coordinates. In case $p = q$, the averaged kernel has a logarithmic singularity, otherwise it is regular. Requiring that the test function v_p and the expansion function w_q have square integrable second and first generalized derivatives, respectively, we transfer the reversed differential operator to v_p. The resulting differential operator incorporates the Helmholtz operator. Together with the periodic boundary conditions, this operator induces a Sturm-Liouville problem for v_p, the eigen functions of which are chosen as test functions. Then, the expansion functions are chosen equal to the test functions. The resulting impedance matrix component is a double integral, which can be rewritten to a single integral in case $p = q$ by use of properties of inner product and convolution.

Choosing a finite number of test and expansion functions on each S_p, we obtain an impedance matrix built up of blocks, which describe the self and mutual coupling of the rings. The blocks on the diagonal are diagonal matrices describing the self coupling of each ring, while the other blocks are dense matrices describing the mutual coupling between each pair of rings. The expansion coefficients are calculated by an LU-factorization of the impedance matrix.

4 Numerical Results

The first result we show is used for validation of the implementation. We show the real and imaginary part of the current through one ring in free space, excited at a frequency of 3 GHz; see Fig. 2. We can compare the result with known results from literature: the current through a wire loop excited by a voltage gap at the same frequency; see [2, Fig. 2 and 3] and [4]. Here, we use a rule of thumb found by Kraus [3, p. 238], which states that the results for a thin strip of width w and a wire with cross-sectional radius $w/4$ are equivalent. Two expansion functions show already an accurate result for the real part of the current. Four expansion functions show a quite accurate result

for the imaginary part of the current, except near the voltage gap in $\vartheta = \pi$. The reason for the latter is the following. It can be shown that since the current has a square integrable generalized derivative, the excitation field should be square integrable. However, the delta functions that describe the voltage gaps are not square integrable. Furthermore, the expansion functions do not only have square integrable generalized derivatives, but are even continuously differentiable.

Figure 3 shows the effect of a ground plate. Figure 3.(a) shows the current amplitude for a ring in free space, and at $h = \lambda/4$, $h = \lambda/2$, and $h = \lambda$ above a ground plate. The current is normalized on the maximum amplitude in free space. Due to interference, the amplitude for $h = \lambda/4$ is lower than for free space, and for $h = \lambda/2$ and $h = \lambda$ higher. Due to space attenuation, the amplitude for $h = \lambda$ is lower than for $h = \lambda/2$. Figure 3.(b) shows the far field components in the yz-plane for free space and for $h = \lambda/4$. Here, a spherical coordinate is chosen that is related to the cartesian coordinate system in Fig. 1 in the usual way. The influence of the ground plate can be observed from the behaviour of the ϕ-component, i.e. the cross-polarization, that vanishes at $\theta = 90^o$ (endfire) for the ground plate, but not for free space.

Figure 4 shows results for two line arrays of 7 identical rings with spacings $7\lambda/15$ and $3\lambda/5$. Here, 8 expansion functions per ring is a suitable choice. The orientation of the local coordinate systems on the rings is such that $\psi_q = 0$. As aforementioned, the voltage gaps, all of equal amplitude, are positioned in $\vartheta_q = \pi$. The centers of the rings are positioned on the positive x-axis, where the center of the first ring is in the origin; see Fig. 1. The CPU time of a Matlab implementation on a HP PC with Windows NT, an Intel Pentium IV processor at 1.6 GHz, and 256 Mb of RAM is 366 sec. Figures 4.(a)-(b) show the normalized radiation intensities in the xz and yz-plane (H and E-plane) together with the intensity of one ring. In the xz-plane, one main lobe and several side lobes are observed for both spacings, where the number of lobes is related to the spacing. In the E-plane, only one lobe is observed. These results are in qualitative correspondence with results from literature; see [1, Chapter 3]. Besides that the array with larger spacing has more side lobes, also its maximal radiation intensity is higher. This effect is due to the degree of mutual coupling. Influence of mutual coupling on the current is shown in Fig. 4.(c)-(f). For smaller spacing, the amplitudes of the currents differ significantly from the amplitude on one ring, while for larger spacing, they differ only slightly. In particular, the maxima of the amplitudes for the spacing $7\lambda/15$ are significantly lower than the maximum for one ring. For the spacing $3\lambda/5$, these maxima are both slightly higher and lower than the maximum for one ring. The phases differ for both spacings from the phase on one ring.

5 Conclusions

We have developed a tool for analysing finite arrays of rings that is easy to handle. The algorithm is based on analytic expressions as required. The validation has been successful; results have shown to be in qualitative correspondence with literature and practice. Although numerically, a brute force method has been applied, the CPU times are acceptable. However, to analyse large arrays of about 100 elements or more, they should be reduced. The accuracy is sufficient for qualitative analysis.

6 Prospects

Research on characteristics of arrays and essential aspects of the antenna elements will be topic of further research. A transparent relation should be established between excitation, geometry, and scattered field. Finally, feedback should be provided to the hardware designers of Thales Nederland.

References

1. Stutzman, W.L., Thiele, G.A.: Antenna Theory and Design. Wiley, New York (1998, 2nd, ed.)
2. Poljak, D.: Finite Element Integral Equation Modelling of a Thin Wire Loop Antenna. Commun. Numer. Meth. Engng. **14** (1998) 347-354
3. Kraus, J.: Antennas. McGraw-Hill, New York (1950).
4. Champagne, N.J., Williams, J.T., Wilton, D.R.: The use of curved segments for numerically modeling thin wire antennas and scatterers. IEEE Trans. Ant. Prop. **40** (1992) 682-688.

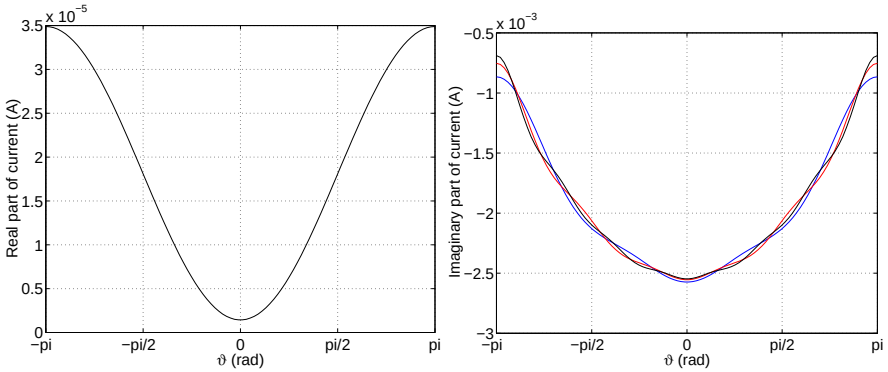

(a) (b)

Fig. 2. The total current on a ring excited by a voltage gap of 1 V at a frequency of 3 GHz.; $a = 0.0637\,\lambda$, $b = 0.0027\,\lambda$, $\mathbf{c} = (0, 0, 0)$, and $\psi = 0$. (a) Real part; 2 expansion functions of cosine type. (b) Imaginary part; blue, red, black: 4, 6, and 8 expansion functions of cosine type.

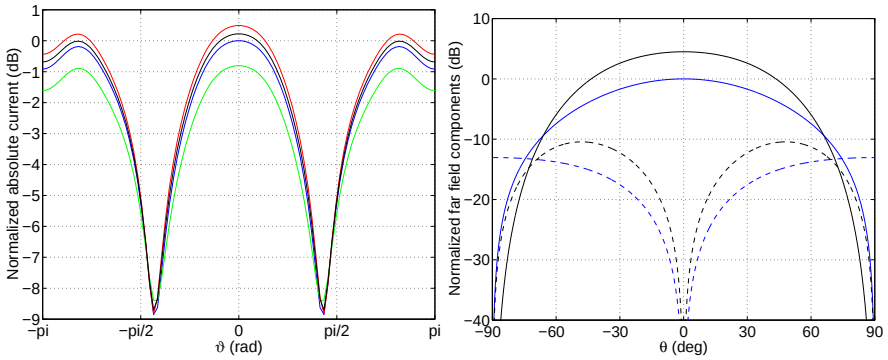

(a) (b)

Fig. 3. A ring excited by a voltage gap of 1 V with 8 expansion functions of cosine type; $ka = 2\pi/5$, $\beta = 1/40$, $\mathbf{c} = (0, 0, 0)$, $\psi = 0$. (a) Current amplitudes normalized on the maximum amplitude in free space; blue: free space; green: $h = \lambda/4$; red: $h = \lambda/2$; black: $h = \lambda$. (b) Far field components in the yz-plane normalized on the maximum of $|E_\theta|$; blue: free space; black: $h = \lambda/4$; solid lines: E_θ-components (co-polarization); dashed lines: E_ϕ-components (cross-polarization).

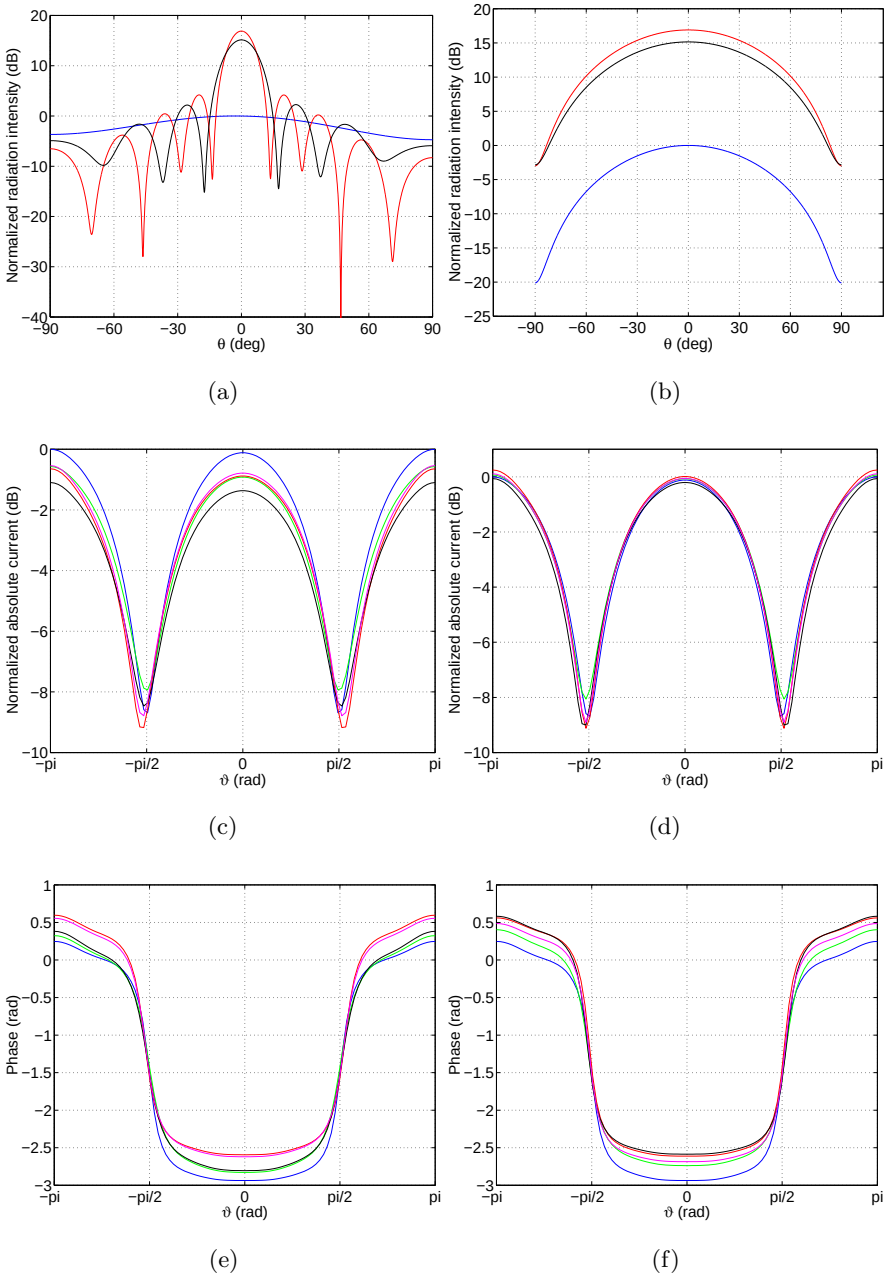

Fig. 4. Results for line arrays of 7 rings of equal radii ($ka_q = 2\pi/6$) and widths ($\beta_q = 3/50$), with voltage gaps of equal amplitude (1 V), and positioned in free space.
(a)-(b): Radiation intensities in the xz and yz-plane, resp., normalized on the maximum intensity of one ring; blue: one ring; black: spacing $7\lambda/15$ ($\mathbf{c}_q = 7\lambda(q-1)/15$); red: spacing $3\lambda/5$ ($\mathbf{c}_q = 3\lambda(q-1)/5$).
(c)-(f): Current amplitudes and phases for spacings $7\lambda/15$ ((c), (e)) and $3\lambda/5$ ((d), (f)); blue: one ring; green/red/black/purple: from first ring to center ring.